Journal of Power Sources 249 (2014) 285–298

Contents lists available at ScienceDirect

Journal of Power Sources

journal homepage: www.elsevier.com/locate/jpowsour

Novel proton exchange membrane based on crosslinked poly(vinyl alcohol) for direct methanol fuel cells

Chien-Pan Liu [a,b,*], Chi-An Dai [b,c], Chi-Yang Chao [d], Shoou-Jinn Chang [a]

[a] Institute of Microelectronics, National Cheng Kung University, Tainan 701, Taiwan
[b] Department of Chemical Engineering, National Taiwan University, Taipei 106, Taiwan
[c] Institute of Polymer Science and Engineering, National Taiwan University, Taipei 106, Taiwan
[d] Department of Materials Science and Engineering, National Taiwan University, Taipei 106, Taiwan

HIGHLIGHTS

- The mechanism of proton transport for bound water phenomenon.
- We examine the water uptake and methanol uptake as a function of IEC for polymer membranes.
- Synergistic effects can enhance the selectivity of the membrane to water/methanol.
- We report the combination of the formula gives the membrane with excellent physicomechanical properties.
- Providing a facile method to fabricate membrane for use as PEMs for DMFCs.

ARTICLE INFO

Article history:
Received 12 March 2013
Received in revised form
24 October 2013
Accepted 25 October 2013
Available online 4 November 2013

Keywords:
Direct methanol fuel cell
Proton exchange membranes
Crosslinked membranes
Proton conductivity
Methanol permeability
Poly (vinyl alcohol)

ABSTRACT

In this study, we report the synthesis and the characterization of poly (vinyl alcohol) based proton conducting membranes. In particular, we describe a novel physically and chemically PVA/HFA (poly (vinyl alcohol)/ hexafluoroglutaric acid) blending membranes with BASANa (Benzenesulfonic acid sodium salt) and GA (Glutaraldehyde) as binary reaction agents. The key PEM parameters such as ion exchange capacity (IEC), water uptake, proton conductivity, and methanol permeability were controlled by adjusting the chemical composition of the membranes. The IEC value of the membrane is found to be an important parameter in affecting water uptake, conductivity as well as the permeability of the resulting membrane. Plots of the water uptake, conductivity, and methanol permeability vs. IEC of the membranes show a distinct change in the slope of their curves at roughly the same IEC value which suggests a transition of structural changes in the network. The proton conductivities and the methanol permeability of all the membranes are in the range of 10^{-3}–10^{-2} S cm^{-1} and 10^{-8}–10^{-7} cm^2 s^{-1}, respectively, depending on its binary crosslinking density, and it shows great selectivity compared with those of Nafion®-117. The membranes display good mechanical properties which suggest a good lifetime usage of the membranes applied in DMFCs.

1. Introduction

The liquid-feed direct methanol fuel cells (DMFCs) have gained much attention on miscellaneous applications because of their lower weight, simple fueling, simple design, low emissions and low temperatures of its low energy conversion efficiency and eco-friendliness [1,2]. In the fuel cell, the proton exchange membrane (PEM) serves as the electrode separator in addition to its primary role as a continuous medium for conducting protons from the anode to cathode [3]. Perfluorosulfonate ionomer membranes, such as Nafion® membranes (DuPont), are the major membranes used in the DMFCs applications presently. However, large-scale applications of these membranes have some drawbacks, limited by their high cost and its unstable properties at high temperature and poor barrier to methanol crossover and difficulty in synthesis and processing [3–5]. Methanol crossover could lower specific cell power output and also reduce the overall efficiency. Therefore, it is very necessary to find novel proton conductive membranes with low cost and low methanol permeability. For this crucial reason, many kinds of PEMs have been successfully developed in recent years; for example, sulfonated aromatic polymers, i.e., polymers with the sulfonic acid groups directly attached to the main chain or carrying

* Corresponding author. Institute of Microelectronics, National Cheng Kung University, Tainan 701, Taiwan. Tel.: +886 912 153973; fax: +886 6 5053669.
E-mail addresses: jasper_liu@epistar.com.tw, e3489236@yahoo.com.tw (C.-P. Liu).

0378-7753/$ – see front matter © 2013 Elsevier B.V. All rights reserved.
http://dx.doi.org/10.1016/j.jpowsour.2013.10.117

short pendant side chains with terminal sulfonic acid units, attract increasing interest because of their chemical and thermal stability, and the ease of the sulfonation procedure. Sulfonated poly(-etheretherketone) (SPEEK) [6,7], sulfonated poly(-etheretherketoneketone) (SPEEKK) [8], sulfonated polyimide (SPI) [9,10], sulfonated poly (benzeneimidazole) (PBI) [11], sulfonated poly(phenylene oxide) (SPPO) [12] have been proposed.

Admittedly, poly (vinyl alcohol) (PVA) has been studied intensively as a membrane because of its good film-forming, highly hydrophilic, and good chemical-resistant properties. In particular, PVA membranes have been used in ethanol dehydration to circumvent the ethanol–water azeotrope because they selectivity pass water molecules over ethanol or methanol [13,14]. However, in order to control water management due to its unstable morphology beneficially as well as surmount the methanol crossover applied further in DMFC thoroughly. There are several ways to crosslink PVA: (1) radiation-induced crosslinking [15,16]; (2) chemical modification of PVA [17–19]; (3) treatments with a multi-functional additive. Especially in (3), they have different methods of treatments using different cross-linking agents. Amalgamating PVA with the additive can get cross-linked by heat treatment when the additive has very low reactivity with PVA under ambient conditions [14,20–22]. If the chemical is able to react with PVA directly, it can lead to cross-linking [23], and plain PVA membranes can also be cross-linked when soaked into a cross-linking medium, gases [24] or liquid solutions [25–27]. Aqueous glutaraldehyde (GA) solution with catalysis is one of the most commonly used cross-linking systems for PVA in the solution of chemical cross-linking techniques. Recently, Pivovar et al. [28] and Rhim et al. [29] reported the preparation of PEMs employing PVA as a base material. Kang et al. reported the preparation of PVA-based (i.e., PVA/poly(styrene sulfonic acid-co-maleic acid (PVA/PSSA-MA)) cation-exchange membranes using blending technique [30,31]. It is reported that the PVA/PSSA-MA membranes exhibit excellent electrochemical properties for electrodialytic separation. Moreover, Qiao et al. reported the preparation of PVA-based (i.e., PVA/poly(2-acrylamido-2-methyl-1-propanesulfonic acid (PVA/PAMPS)) cation-exchange membranes exhibit excellent proton conductivity and better mechanical property although both IEC and WU are much higher than that of Nafion®-117 [32–34].

In this study, we prepared the PVA/HFA (poly (vinyl alcohol)/hexafluoroglutaric acid) physically and chemically membranes with BASANa (Benzenesulfonic acid sodium salt) and GA (Glutaraldehyde) as binary reaction agents. Our strategy is to use HFA combined with dicarboxylic acid as the thermal cross-linking agent into PVA and enhanced the flexibility by blending technique; namely, the synergistic effects can enhance the affinity of the membrane to water because the carboxylic group has a relatively high polarity and a strong interaction with water through hydro bonding, showing superior water managing ability than methanol. In addition, we also use GA with dialdehyde as the chemical cross-linking reaction into PVA chains when PVA/HFA membranes soak into a cross-linking medium with GA. Particularly, We choose BASANa with both aldehyde group and sulfonic acid group, taking as the pedant side chains on cross-linked PVA and molecularly separated from the hydrophobic backbone.

2. Experimental section

2.1. Materials

Fully hydrolyzed poly(vinyl alcohol), PVA, (99% hydrolyzed, average M_w = 89,000–98,000) was purchased from Aldrich Chemical Co., USA. All other chemicals, including hexafluoroglutaric acid (HFA, 97%), glutaraldehyde (GA 50% solution), benzaldehyde-2-sulfonic acid sodium salt (BASANa, 90%, tech.), phenolphthalein (indicator grade, pure), acetone (99%), dilute hydrochloric acid (30%) and sulfuric acid (98%) were obtained from Acros Co., USA. *N*,*N*-Dimethylformamide (DMF) and methanol (MeOH) used were also purchased from Aldrich, and were of analytical grade. The water used was distilled and deionized water.

2.2. Membrane preparation

The polymer membranes were formed by solution casting method. Aqueous 10 wt.% PVA (poly vinyl alcohol) solutions were prepared by dissolving dry PVA in deionized water at 80 °C for 6 h, by stirring vigorously until a translucent solution was obtained and then cooled to room temperature. Furthermore, another aqueous 20 wt.% HFA (Hexafluoroglutaric acid) solutions were prepared at room temperature. These two solutions amalgamated together by varying each component composition to form a homogeneous solution for 1 h. The selected polymer composition of PVA/HFA was 2:1, 2:2, 2:3 (in mass). The PVA/HFA well-mixed solution was degassed using a vacuum pump over a period of 4 h. After that, the cooled and degassed solutions were poured and cast onto plastic petri dishes, dried under ambient conditions (temperature 25 °C) in air for more than 2 days. When visually dry, the resulting dried membranes were then annealed at 120 °C for 30 min to further induce physical cross-linking reaction in a thermoset oven. Subsequently, the membranes were peeled off from plastic petri dishes and prepared to the next chemical treatment.

'In the chemical treatment facet, the binary reaction agents of the chemical cross-linking solution separately consisted of "2-Formylbenzenesulfonic acid sodium salt (BASANa), DMF, a catalyst dilute HCl" as well as "glutaraldehyde (GA), acetone, a catalyst H_2SO_4", these two reaction solutions were marked as "BmGn" in different content of concentration. Samples of polymer membranes were cut into square pieces about 3 cm × 3 cm, soaking individually in above two steps of reaction solution "BmGn" for each 3 h at room temperature. The cross-linking reaction was taken place between the hydroxyl groups of PVA and aldehyde groups of reaction solution "BmGn" in the membrane owing to an acid-catalyzed reaction by HCl or H_2SO_4. The postulated reaction mechanism of physically cross-linked PVA-HFA blend membranes and chemically cross-linked PVA-HFA-BASANa membranes are illustrated in Fig. 1, this kind of membranes are to be used in our subsequent research. In all cases, after chemical cross-linking reaction, the membranes were taken out, washed with water several times and finally immersed in deionized water for 6 h to eliminate residual acid oozed from the membranes. Afterward, again, taken out and stored in deionized water for final proton conductivity measurements. The thickness of membranes was in the range of 100–250 μm. In this study, we prepared chiefly different chemical cross-linking solutions, we designated as BmGn. For instance, B3G6 indicates the 2-Formylbenzenesulfonic acid sodium salt (BASANa)/glutaraldehyde (GA) binary cross-linking agent with the composition of 3 wt.% and 6 wt.% in DMF and acetone solution, respectively, et cetera.

2.3. The swelling properties of the membranes

The membrane swelling towards pure water and methanol was determined in terms of conventional liquid uptake and the number of liquid molecular per sulfonic acid groups. The liquid uptake, including methanol uptake (MU) and water uptake (WU), was determined in the following way: at first the membrane samples were dried under vacuum for 1 h at 80 °C and then weighed. They were then soaked in deionized water or 40 wt.% methanol overnight until swelling equilibrium was achieved, then the surface-attached liquid on both sides was carefully blotted

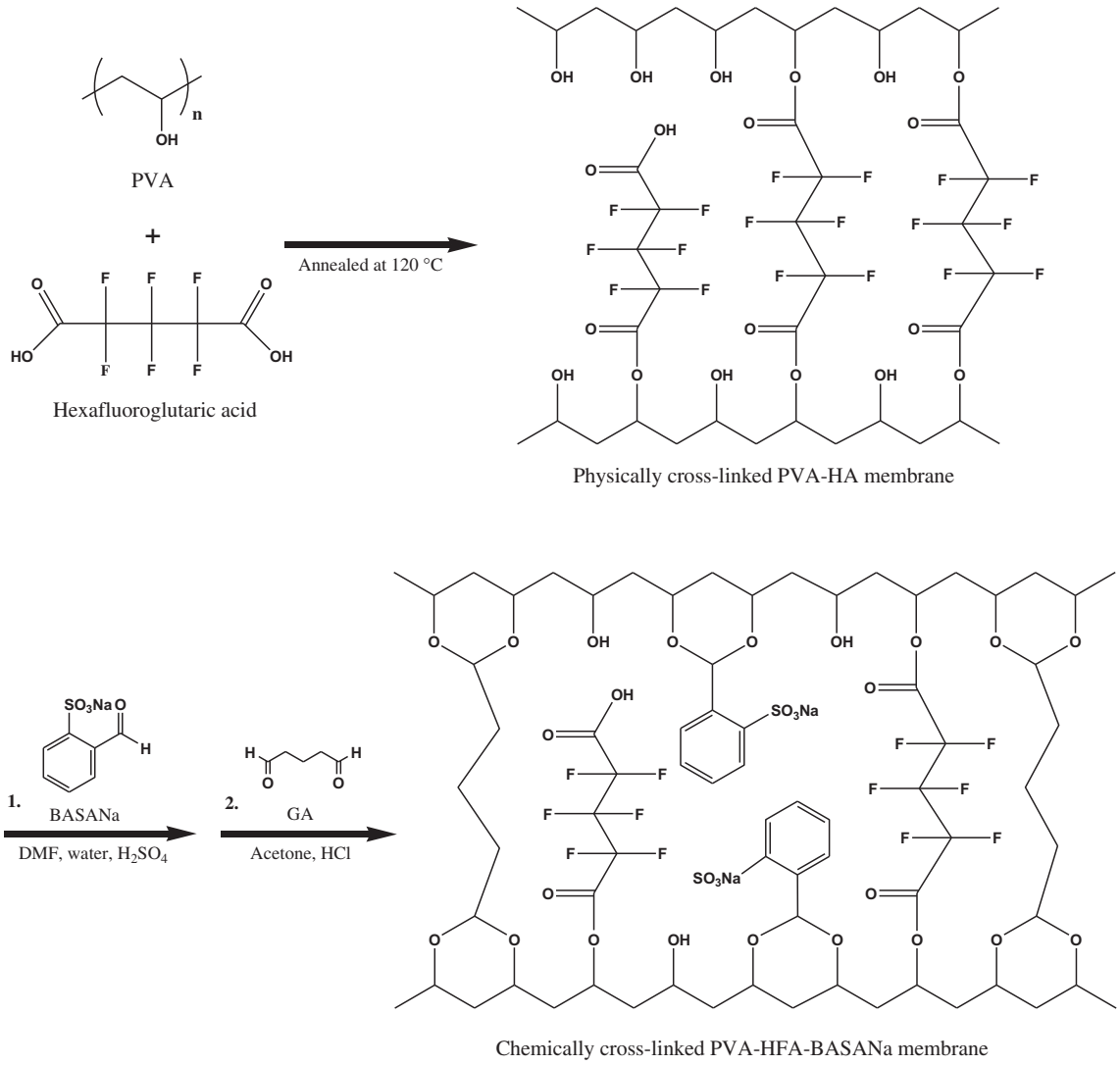

Fig. 1. Possible reaction mechanism of physically cross-linked PVA/HFA membranes and chemically cross-linked PVA-HFA membranes in different binary reaction agents for BmGn. Here PVA served as cross-linking network; GA and HFA as cross-linking agent; BASANa as a proton conductor.

with a filter paper, and they were immediately weighed. The methanol uptake and water uptake were conducted measuring the weight differences between the fully-hydrated membranes and the dried membranes. They were calculated by the following expression:

$$\mathrm{MU}(\%) = \frac{W_{\mathrm{swollen}} - W_{\mathrm{dry}}}{W_{\mathrm{dry}}} \times 100 \tag{1}$$

$$\mathrm{WU}(\%) = \frac{W_{\mathrm{swollen}} - W_{\mathrm{dry}}}{W_{\mathrm{dry}}} \times 100 \tag{2}$$

where W_{swollen} is the weight of methanol (or water)-swollen membranes and W_{dry} the weight of the dry membranes.

The number of the sorbed liquid molecules (methanol or water) per ionic site (λm orλw) was calculated using the following equations [35]:

$$\lambda_{\mathrm{m}} = \frac{\mathrm{MU}}{M(32) \times \mathrm{IEC}} \times 1000 \tag{3}$$

$$\lambda_{\mathrm{w}} = \frac{\mathrm{WU}}{M(18) \times \mathrm{IEC}} \times 1000 \tag{4}$$

where MU and WU are the weight of the methanol uptake and water uptake of the membrane samples, which are obtained from Eq. (1) and (2) and where M the molecular weight of the considered liquid, IEC are mentioned below.

2.4. Ion exchange capacity

The ion exchange capacity (also known as the IEC value) of the membranes was determined the classical titration technique. Firstly, square pieces of each membrane were soaked in a large volume of 1 M HCl solution and heated to 70 °C for 1 h, which changed them into the H^+ form. The samples were then washed with distilled water several times to remove excess HCl, right after that soaked them in boiling water for 1 h which confirmed the stability of membranes in hydrolytic condition. Next step, we take the samples in 50 ml of 1 M NaCl solution heated to 40 °C and equilibrated for at least 24 h to replace the protons by sodium ions. The remaining solution was titrated with 0.01 N NaOH solution using phenolphthalein as an indicator. The IEC value

(mmol g^{-1} (meq g^{-1})) was calculated using the following equation:

$$\mathrm{IEC} = \frac{0.01(V_O - V_E)}{W_{dry}} \quad (5)$$

Where V_O is the volume of NaOH in the flask at the beginning of the titration, V_E is the volume of NaOH after equilibrium, and W_{dry} is the weight of the dry membrane (g).

2.5. Wide- and small- angle X-ray scattering (WAXS and SAXS) measurements; atomic force microscopy (AFM) observations

WAXS experiments were examined using a X'Pert Wide-angle X-ray diffraction (WAXD) with Cu Kα radiation of wavelength $\lambda = 1.5418367$ Å for 2θ angles between 10° and 70°. The X-ray generator was operated at excitation voltage of 40 kV and a current of 100 mA. Besides, SAXS measurements were performed on beamline 17B3 of the National Synchrotron Radiation Research Center (NSRRC), Taiwan. Measurements were carried out for membrane samples in water-swollen state. All samples were kept in sealed polyimide envelopes during the measurements.

Phase-lag atomic force microscopy (AFM) images were measured with a Digital Instrument (DI) BioScope SZ under tapping mode. The oscillation frequency was set to approximately 295 kHz with Si cantilever which had a force constant of about 40 N m^{-1}. All samples were measured under room temperature and relative humidity of 40%.

2.6. Proton conductivity

Proton conductivity was determined by an electrochemical (or AC) impedance spectroscopy (EIS) taken between 100 kHz and 0.1 MHz at a voltage amplitude of 10 mV using an impedance/gain-phase analyzer (Solartron 1260, Solatron Analytical, UK) in combination with an electrochemical interface (Solartron 1287). A homemade two-point probe electrode method (through the plane of the membrane) was employed using a test fixture measured the proton conductivity of the membranes, the cell geometry which was mentioned in our previous work [36]. The testing device with the membrane was immersed in deionized water and placed in a thermostatically controlled chamber at temperature ranging from 25 to 100 °C. The proton conductivity (σ) was obtained using the following equation:

$$\sigma = \frac{l}{R \cdot A} \quad (6)$$

where σ is the proton conductivity (Scm^{-1}) and l is the thickness of the membrane (cm). R is the bulk resistance or ohmic resistance of the membrane sample (Ω). A is the contact area required for a proton to penetrate the membrane (cm [2]). The impedance of each sample was measured at least five times to ensure good data reproducibility.

2.7. Mechanical property

Mechanical tensile tests were performed using an Universal Testing Machine (Yashima Works Ltd. Co., model RTM-IT) at room temperature, with an operating head load of 5 kN. The gauge lengths were all set to 30 mm and the crosshead displacement speed of testing was set at the rate of 5 mm min^{-1}. The specimens with thickness around 200 μm and size of 60 mm × 30 mm were used for testing. It was possible to determine a modulus of elasticity or so called Young's modulus (E) in the elastic portion of the stress–strain curve by Hooke's law. Tensile strength (TS) is the stress at the maximum in the plastic portion of the stress–strain curve that may be sustained by a specimen. Tensile strength was calculated using:

$$\mathrm{TS(tensile\ strength,\ MPa)} = \frac{F(\mathrm{max\ load,\ N})}{A_0(\mathrm{cross-section\ area,\ mm^2})} \quad (7)$$

In addition, ductility is another important mechanical property. It is a measure of the degree of plastic deformation that has been sustained at fracture. Ductility may be expressed quantitatively as percent elongation (% EL), which was the percentage of plastic strain at fracture and calculated from:

$$\%\mathrm{EL} = \left(\frac{l_f - l_0}{l_0}\right) \times 100 \quad (8)$$

where l_f is the fracture length and l_0 is the original gauge length as above.

Membrane toughness level by the bending test was carried out for a membrane sheet 5 mm in wide and 20 mm in length at room temperature. The membrane toughness level was set as follows. In level I, the membrane is brittle and breaks into pieces by handling. In level II, the membrane sheet breaks when it is bent by holding both ends between fingers. In level III, the membrane sheet breaks along a fold when it is folded to zero degree. In level IV, the membrane sheet breaks when it is folded back. In level V, the membrane sheet does not break after it is folded back [37].

2.8. Methanol permeability

Typically, a transport phenomenon in PEMs as small molecules across a dense (nonporous) polymer membrane follows a solution-diffusion mechanism. The methanol permeability of the membranes was determined using a diaphragm diffusion cell method [28]. Basically, this glass cell consisted of two reservoirs each approximately 60 ml, separated by a vertical membrane. The membrane (effective area 3.14 cm^2) was fixed and clamped between both reservoirs. Initially, one reservoir (V_A) was filled with a 40 ml of 50 vol% methanol solution in distilled water, and the other reservoir (V_B) was filled with pure deionized water. Methanol permeates across the membrane by the concentration difference between the two reservoirs. We can measure the concentration of methanol by density/concentration meter (DMA4500, Anton Paar, Austria), then the methanol concentration in the receiving reservoir as a function of time is given by the following equation:

$$C_B = \frac{A}{V_B}\frac{DK}{l}[C_A(t_0)](t - t_0) \quad (9)$$

where C_B is the concentration of methanol in the water reservoir as time goes by, C_A the methanol concentration in the methanol reservoir, A (cm [2]) the effective area of membrane, l (cm) the membrane thickness, V_B the volume of water in its reservoir, D the methanol diffusivity and K is the partition coefficient between the membrane and the adjacent solution. The product DK means the membrane permeability (P_M):

$$P_M = DK = \frac{1}{A}\frac{C_B(t)}{C_A(t_0)}\frac{V_B l}{t - t_0} \quad (10)$$

Parameter t_0 is the lag time and correspond to the time necessary for the methanol to pass through the membrane. C_B here is measured several times during the permeation experiment and the methanol permeability is obtained from the slope of equation (10).

2.9. Hydrolytic stability and oxidative stability

In the present study, it has performed the hydrolytic stability test. The PVA/HFA (2/2) chemically cross-linked membranes in different binary reaction agents for B15Gn (*n* from 2 wt.% to 10 wt.%) immersed in 60 °C deionized water for 1 week. The proton conductivity and IEC were measured before and after the hydrolytic stability tests. In addition, we have also performed the oxidative stability test. The PVA/HFA (2/2) chemically cross-linked membranes in different binary reaction agents for B15Gn (*n* from 2 wt.% to 10 wt.%) were immersed in Fenton's reagent (10 wt.% H_2O_2 solution containing 5 ppm $FeSO_4$) at room temperature. The variation of weight loss was measured with elapsed time and times were recorded from commencement to break of samples in Fenton's reagent.

3. Results and discussion

3.1. FT-IR/ATR spectra characterization

The FT-IR/ATR spectra of the membranes were examined by FT-IR (480 plus, Jasco, Japan) equipped with an ATR accessory. It measured for both top and bottom surfaces, including the fresh PVA film, heat-treated PVA film, the PVA/HFA (2/2) physically cross-linked membrane and the PVA/HFA (2/2) chemically cross-linked membrane in binary reaction agent for B15G4 which were presented in Fig. 2a. The FT-IR/ATR spectrum of the fresh PVA film shows the very strong broad peak at ~3270 cm^{-1} for the intermolecular hydrogen bonding and the hydroxyl (O–H) stretching vibration. The C–H asymmetrical and symmetrical stretching vibration occurs at 2940 cm^{-1} and 2910 cm^{-1}, respectively. The two transmission peaks at 1712 cm^{-1} and 1093 cm^{-1} is attributed to the stretching vibration of C=O and C–O of the remaining non-hydrolyzed vinyl acetate group of the PVA [14]. Another two transmission peaks at 1415 cm^{-1} and 1328 cm^{-1} is due to –C–H– and –O–H– bending [38]. The peak at 1328 cm^{-1} is attributed to the C–H wagging vibrations.

Heat treatment of PVA results in the elimination of water and hence there is a fall in hydroxyl content, which is reflected by a comparatively narrower band compared with the fresh PVA film, centered at 3278 cm^{-1}. Besides, the other transmission peaks are similar to the fresh PVA film.

The FT-IR/ATR spectra of the PVA/HFA physically cross-linked membranes shows the transmission peak at 1764 cm^{-1} which is due to –C=O stretching vibration with $-CF_2COOH$ group for HFA. The intensity of the –C=O in the ester bond increases with the amount of the PVA/HFA weight ratio in the range of 2/1–2/3 (Fig. 2b). The transmission peak at 1246 cm^{-1} arose from the C–O stretching mode in the ester group. The transmission peak at 914 cm^{-1} is the O–H out-of-plane motion of the carboxylic group in the HFA. While the C–O stretching mode increases with the amount of HFA, the intensity of the O–H out of plane motion is reduced owing to further thermally cross-linked reaction (Fig. 2b). From these results, the spectral changes are an evidence of a cross-linking by the esterification between –OH in PVA and –COOH in HFA, depending on the amount of the cross-linking agent at the same temperature. In addition, we can also find the two transmission peaks at 1170 cm^{-1} and 1145 cm^{-1} attributed to the C–F groups from HFA, and the intensity of C–F groups is also increased owing to increasing the amount of HFA. Here we chose the PVA/HFA (2/2) physically cross-linked membrane in comparison with the other polymer membranes in Fig. 2a.

The FT-IR/ATR spectra of the PVA/HFA (2/2) chemically cross-linked membrane in binary reaction agent for B15G4 shows the transmission peak at 2866 cm^{-1} and 1717 cm^{-1}, these two peaks

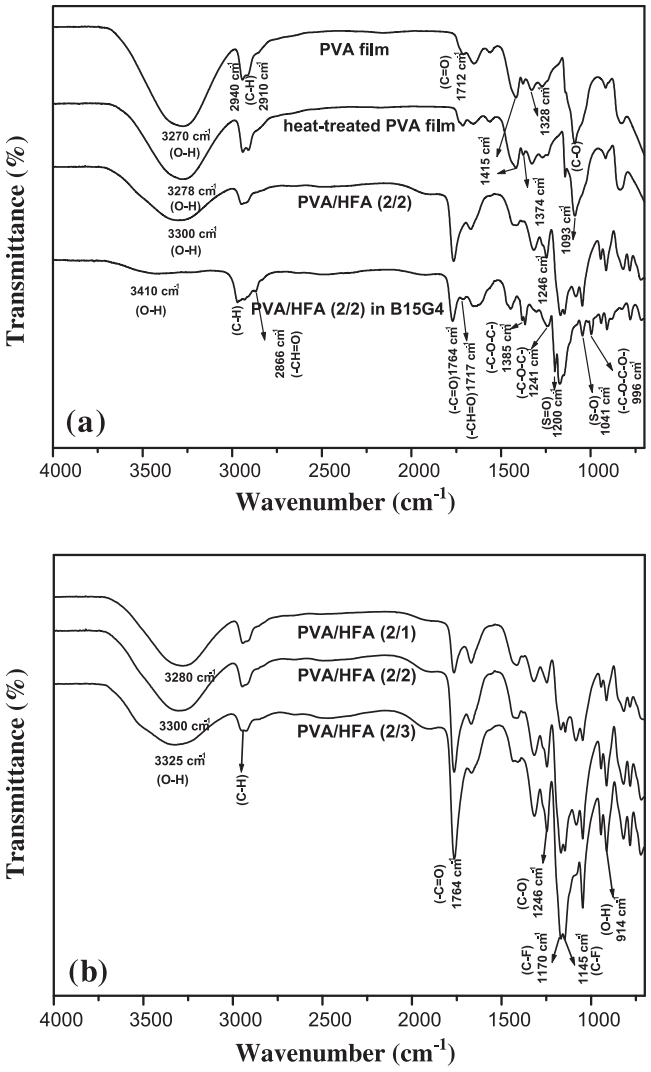

Fig. 2. (a) FT-IR/ATR spectra of the fresh PVA film, heat-treated PVA film, and the PVA/HFA (2/2) physically cross-linked membrane and the PVA/HFA (2/2) chemically cross-linked membrane in binary reaction agent for B15G4. (b) The PVA/HFA physically cross-linked membrane, where PVA/HFA weight ration from 2/1 to 2/3.

are attributed to the characteristics of the aldehyde group (–CH=O) from GA. Another two additional transmission peaks appear at 996 cm^{-1} and 1385 cm^{-1}, which arise from formed acetal group (–C–O–C–O–) and ether linkage (–C–O–C–) as a result of the reaction between the hydroxyl groups and the aldehydes in the polymer network [39,40]. The peak at 1041 cm^{-1} is also clearly observed due to the S–O stretching of sulfonate group [33]. The strong peak at 1200 cm^{-1} is ascribed to S=O asymmetric vibration of sulfonic acid groups [9]. From this result, it can demonstrate that the binary reaction agents facilitate theirs diffusion in PVA/HFA blending membranes by proper solvent, and they react with PVA to form acetal or ether groups for cross-linking or dangling in the polymer network. In comparison with the O–H peak of fresh PVA film (3270 cm^{-1}), the O–H peak of the PVA/HFA (2/2) physically cross-linked membrane and the PVA/HFA (2/2) chemically cross-linked membrane in binary reaction agent for B15G4 shifts to higher wavelength reaction (3300 cm^{-1} and 3410 cm^{-1}). This phenomenon also found in different PVA/HFA weight ratio in the range of 2/1–2/3 (Fig. 2b). It indicates that the formation of hydrogen bonds among –OH of PVA, –COOH of HFA and $-SO_3H$ of BASANa occurs and the interaction between –OH groups of PVA is

stronger than that among −OH, −COOH and $-SO_3H$. In brief, it suggesting that the hydrogen bonding between −OH groups of PVA becomes weaker in chemically cross-linked PVA/HFA (2/2) that in fresh PVA or thermally cross-linked PVA/HFA due to the diminution in the number of −OH groups [30,41].

3.2. Morphological analysis

The morphological examination of the prepared membranes was performed through FE-SEM. Fig. 3 shows the FE-SEM cross-section image of the prepared fresh PVA film, the PVA/HFA (2/1, 2/2) thermally cross-linked membrane and the PVA/HFA (2/2) chemically cross-linked membranes in different binary reaction agents for B15Gn (n from 6 wt.% to 10 wt.%). It is interesting to observe very distinct features in all six cases. The fresh PVA film shows a distinct layered morphology and the thermally cross-linked PVA/HFA (2/1) membrane is somewhat similar to fresh PVA but has a half of layered morphology. Nevertheless, thermally cross-linked PVA/HFA (2/2) membrane is quite different from the above. It shows a flat-type morphology, which results in not only the elimination of water but the addition of more HFA in the PVA network. It also causes ostensible smooth on the membrane surface, the cross-section dense and its uncreased layer is proved that the PVA and HFA blend well. In addition, the PVA/HFA (2/2) chemically cross-linked membranes shows the honeycomb-type morphology and arises with GA soaking medium content. The polymer membranes make less hydrophilic via a series of thermal cross-linking and chemical cross-linking reactions. The results also echo with the room mean square (RMS) roughness in the AFM image analysis as well as in contact angle experiment, having the same trend as mentioned above; as shown in Table 1, the more roughness of the membranes due to its cross-linking degree, the more advancing contact angle (θ_a) due to the decreasing in −OH group from PVA. Consequently, the interlocking of the chains results in a comparatively “closed structure” and have more hydrophobic domains.

3.3. TGA thermal analysis and degradation

Thermogravimetric analysis was conducted in a nitrogen atmosphere from 50 to 700 °C at a heating rate of 10 °C min^{-1}. Fig. 4 shows TGA analysis of the PVA polymer membrane alone, the PVA/

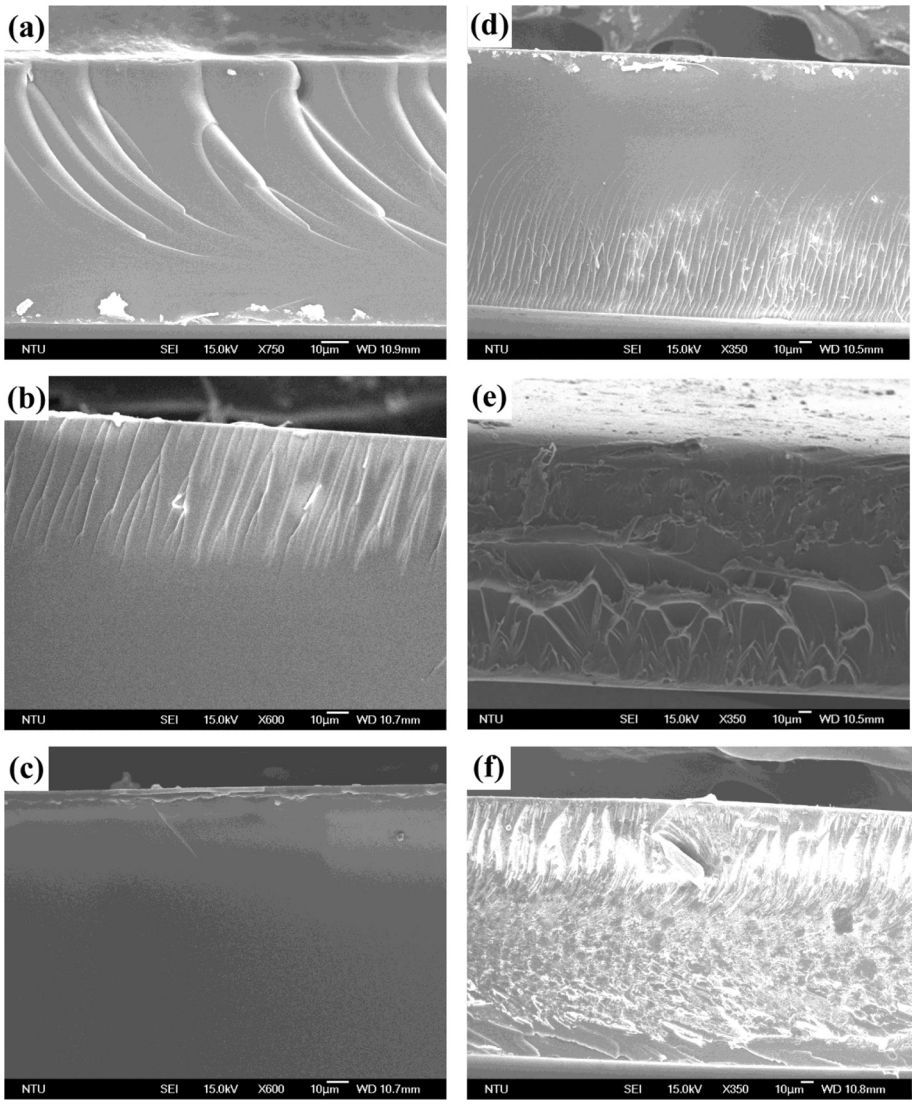

Fig. 3. FE-SEM cross-section image of the (a) fresh PVA film; the PVA/HFA physically cross-linked membrane, where the weight ratio of (b) PVA/HFA = 2/1 and (c) PVA/HFA = 2/2; the PVA/HFA (2/2) chemically cross-linked membranes in different binary reaction agents for B15Gn, where (d) n = 6, (e) n = 8 and (f) n = 10 of GA wt.%.

Table 1
Results of polymer membranes from AFM experiments and contact angle experiments at room temperature.

Membranes	Maximum peak-valley, R_{p-v} (nm)	RMS roughness, R_q (nm)	Advancing contact angle, θ_a (°)
PVA film	6.059	1.140	73.42
PVA/HFA (2/2)	2.990	0.730	74.17
PVA/HFA (2/2) in B15G2	6.643	1.272	76.56
PVA/HFA (2/2) in B15G4	7.530	1.681	78.21
PVA/HFA (2/2) in B15G6	11.969	2.345	79.34
PVA/HFA (2/2) in B15G8	13.686	2.540	81.15
PVA/HFA (2/2) in B15G10	46.775	3.481	83.67

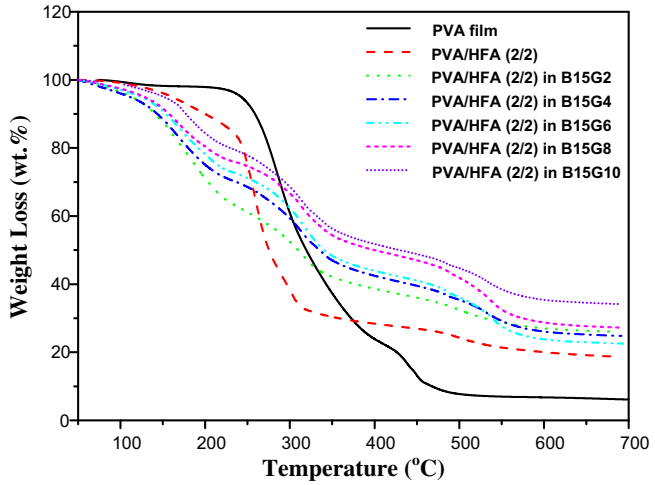

Fig. 4. TGA curves of the fresh PVA film, the PVA/HFA (2/2) physically cross-linked membrane and the PVA/HFA (2/2) chemically cross-linked membranes in different binary reaction agents for B15Gn (n from 2 wt.% to 10 wt.% of GA).

HFA (2/2) physically cross-linked membrane and the PVA/HFA (2/2) chemically cross-linked membranes in different binary reaction agents for B15Gn (n from 2 wt.% to 10 wt.%) in this work, respectively. TGA curves of the plain PVA polymer film reveal three main weight loss regions, which appear as three peaks in the derivative thermogravimetric (DTG) (not provided). The first region at a temperature of 90–110 °C is due to the evaporation of physical weakly bound water; the weight of the membrane is about 99.25 wt.%. The second transition region at around 250–400 °C is due to the degradation of PVA polymer membrane; the total weight corresponds to this stage about 71.27 wt.%. The third transition region at around 400–500 °C is due to the cleavage backbond of PVA polymer membrane (or so-called carbonation); the residual ash is 6.11 wt.% at 700 °C, as listed in Table 2.

Table 2
The thermal property of the fresh PVA film, the PVA/HFA (2/2) physically cross-linked membrane and the PVA/HFA (2/2) chemically cross-linked membranes in different binary reaction agents for B15Gn (n from 2 wt.% to 10 wt.%) by TGA analysis.

Membranes	$T_{d5\%}$ (°C)[a]	T (°C)[b]				Ash[c]
		150	250	350	500	
PVA film	242.5	98.23	93.18	37.29	7.74	6.11
PVA/HFA (2/2)	160.65	96.09	74.93	30.39	24.24	18.72
PVA/HFA (2/2) in B15G2	113.92	87.62	61.17	42.16	32.41	26.00
PVA/HFA (2/2) in B15G4	111.17	88.46	68.54	47.01	35.43	24.79
PVA/HFA (2/2) in B15G6	124.17	90.86	71.17	48.33	36.12	22.55
PVA/HFA (2/2) in B15G8	127.99	91.61	74.65	54.35	41.87	27.25
PVA/HFA (2/2) in B15G10	151.00	95.12	77.83	56.29	44.74	34.14

[a] 5 wt.% weight loss temperature.
[b] The weight at every single temperature.
[c] Residual ash is the char yield (wt.%) at the 700 °C.

Furthermore, the TGA curve of the PVA/HFA (2/2) physically cross-linked membrane also display three main weight losses. The first stage at a temperature range of 90–150 °C is also due to the removal of bound water; the weight is about 97.56 wt.%. As a matter of fact, the second transition at around 250–350 °C is due to the degradation of PVA blending membrane; the total weight corresponds to this stage about 66.91 wt.%. Obviously, the second main weight loss is much more intense, compared with the pure PVA polymer film. The third transition region at around 470–520 °C is due to the breaking main chains of PVA polymer membrane; there is a total weight of residual ash at 700 °C about 18.72 wt.%.

Moreover, the TGA curves of the PVA/HFA (2/2) chemically cross-linked membranes in different binary reaction agents for B15Gn (n from 2 wt.% to 10 wt.%) was fitted using three main degradation stages arising from the processes of thermal salvation, thermal desulfonation, and thermal oxidation of the polymer matrix. Similar effects were also observed in PVA/PSSA_MA proton-conducting systems [30]. The first stage at a temperature range of 100–230 °C is also due to the removal of bound water; the bound water seems to be bound directly to the PVA polymer chains and/or the $-SO_3H$ groups via hydrogen bonds. The $T_{d5\%}$ and the weight of polymer membranes in this stage increase with increasing the soaking medium of GA content. The second transition region at around 240–375 °C is due to the loss of sulfonic acid group by thermal desulfonation. The second main weight loss degree of the PVA/HFA (2/2) chemically cross-linked membranes apparently lower than the PVA/HFA (2/2) physically cross-linked membrane with increasing the soaking medium of GA content. However, the weight loss of the polymer membranes in the second region is still more than PVA polymer film, resulting from the addition of sulfonic acid group. In the third transition region at around 460–600 °C corresponds to the decomposition of the main chains of PVA polymer membrane. The weight remaining after the polymer decomposition depended on the soaking medium of GA content.

Overall, the weight residue of polymer membranes increase with increasing the soaking medium of GA content due to the higher degree of crosslinking. An increase in GA content induces more crosslinking in the PVA matrix, which leads to an increase in the residual char formed at $T = 700$ °C. It can be concluded that the improved thermal stability is probably due to combining thermal-crosslinking and chemical-crosslinking reaction of among PVA, HFA and GA.

3.4. Differential scanning calorimetry

The DSC measurements was conducted in a nitrogen atmosphere from −50 to +250 °C at the heating rate of 10 °C min^{-1} in hermetically sealed aluminum pans. The second heating curve was evaluated. The results of DSC thermograms of the PVA/HFA (2/2) chemically cross-linked membranes in different binary reaction agents for B15Gn (n from 2 wt.% to 10 wt.%) are plotted in Fig. 5. The only phase transition observed in the −50 to 50 °C temperature range is the glass transition temperature T_g after the membrane was

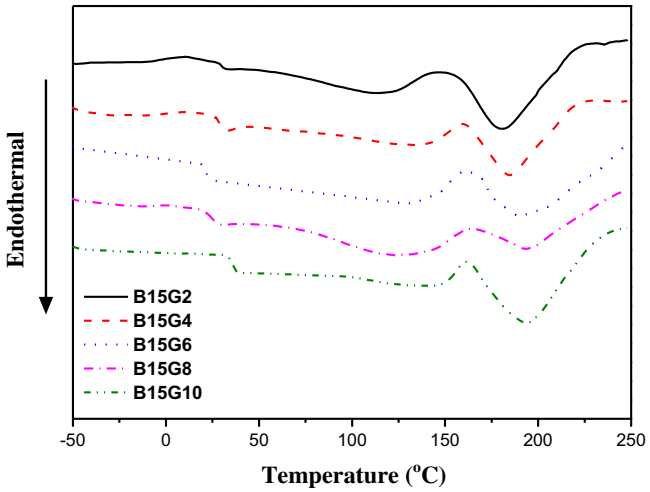

Fig. 5. DSC curves of the PVA/HFA (2/2) chemically cross-linked membranes in different binary reaction agents for B15Gn (n from 2 wt.% to 10 wt.% of GA).

chemically modified. Above this temperature a series of peaks appeared that was probably due to the loss of water and the onset of the thermal decomposition of BASANa just as the TGA profiles showed. In this work, the T_g of pristine PVA was found to be at 78 °C, which is in agreement with the result reported elsewhere [42]. Therefore, this sharp reduction of glass transition temperature to around 25–35 °C (Fig. 5.) could be explained by the plasticizing effect of BASANa (or SO_3H groups) and the cross-linking (HFA) on the PVA matrix, such plasticization normally increases polymer flexibility or mobility, including water molecules absorbed into a polymeric matrix; however, changing the GA compositions presented no distinct differences in glass transition temperatures. Besides, exothermic peaks are observed which is associated with the cold crystallization transition; the endothermic peak may be attributed to the melting of polymer crystallizes that have been formed before [42]. These endothermic and exothermic responses were observed around 160–190 °C except for the expulsion of water molecules from the polymer matrices. Combined with the results of the TGA provided, the PVA/HFA (2/2) chemically cross-linked membranes in different binary reaction agents are considered to be thermally stable up to 180 °C in dry nitrogen. These results show a general trend that higher crosslinked polymer matrix exhibit better thermal stability.

3.5. The swelling properties of the membranes and ion exchange capacity (IEC)

The swelling property and IEC are well known to have the profound effects on the proton conducting polymer membranes. The liquid uptake and IEC values of the polymer membranes were measured by gravimetry and neutralization titration, respectively, and the results are shown in Table 3. Before chemical cross-linking, all of the PVA/HFA physically cross-linked membrane samples could be not stable in water and could be too pliable for a long time. Therefore, only thermal cross-linking technique is not enough for applying in proton exchange membrane. Chemical cross-linking is an effective means for overcoming this effect. Just as described in the Experimental Section, the chemical cross-linking in pristine PVA/HFA with GA as a cross-linker to form the main chain gives the polymer membrane a good mechanical property and the flexibility of the membranes was also achieved at the same time. From Fig. 6a, PVA has good methanol control but has poor water control as its physical property; besides, the PVA will get along with the augmentation of the HFA showing superior water managing ability than methanol, so the PVA/HFA physically cross-linked membrane of their difference between WU and MU become more and smaller to control to some limited grades depending on different cross-linking reaction agents. Consequently, these fluorine-containing polymers generally show lower water uptake than non-fluorinated analogs because of the fluorine atoms confer a strong C–F bond contributing good chemical resistance and thermo-oxidative stability [43]. Furthermore, the water uptake of the PVA/HFA (2/2) chemically cross-linked membranes increased gradually with BASANa content due to the strong hydrophilicity of the sulfonic acid groups, and the IEC also increased with increasing BASANa content in soaking medium. However, it should be noticed that the water uptake and IEC decreased almost linearly with the soaking medium content of GA. This inversely phenomenon due to the glutaraldehyde (GA) functioned as a hydrophobicizer and the

Table 3
The IEC, liquid uptake (MU and WU), the state of water, and number of liquid molecules per ionic site (—SO_3H) in different polymer membranes compared with those of Nafion®-117.

Membranes	IEC (meq g^{-1})	MU[a] (%)	WU[b] (%)	FW[c] (%)	BW[d] (%)	λ_m[e]	λ_w[f]
PVA film	0.012	12.43	317.13	244.58	72.55	323.70	14681.9
PVA/HFA (2/1)	0.115	26.18	257.46	154.48	102.98	71.14	1243.77
PVA/HFA (2/2)	0.188	37.44	209.25	117.28	91.97	62.23	618.35
PVA/HFA (2/3)	0.254	42.32	170.68	88.67	82.01	32.21	563.12
PVA/HFA (2/2) in B3G6	0.381	11.89	33.12	12.21	20.91	9.75	48.29
PVA/HFA (2/2) in B6G6	0.454	16.64	45.86	15.58	30.28	11.45	56.12
PVA/HFA (2/2) in B9G6	0.567	21.73	58.37	18.68	39.69	11.98	57.19
PVA/HFA (2/2) in B12G6	0.786	30.17	86.18	24.67	61.51	12.00	60.91
PVA/HFA (2/2) in B15G6	0.942	37.04	105.26	25.31	79.95	12.29	62.08
PVA/HFA (2/2) in B20G6	1.225	49.26	171.72	41.89	129.83	12.57	77.88
PVA/HFA (2/2) in B15G2	1.158	48.36	160.86	38.77	122.09	13.05	77.17
PVA/HFA (2/2) in B15G4	1.078	43.46	125.37	30.18	95.19	12.60	64.61
PVA/HFA (2/2) in B15G8	0.818	31.12	61.05	14.69	43.36	11.89	41.46
PVA/HFA (2/2) in B15G10	0.632	22.83	25.12	6.01	19.11	11.29	22.08
Nafion®-117	0.9	76.37	33.4	7.75	25.65	26.52	37.11

[a] Methanol uptake.
[b] Water uptake or total water content.
[c] Free water, which is calculated from the DSC analysis. Here, the heat of fusion of pure ice (334 J g^{-1}) was used for evaluating the degree of crystallinity from the melt endotherm in DSC thermograms.
[d] Bound water = total water content-free water.
[e] λ_m: number of methanol molecules per ionic site.
[f] λ_w: number of water molecules per ionic site.

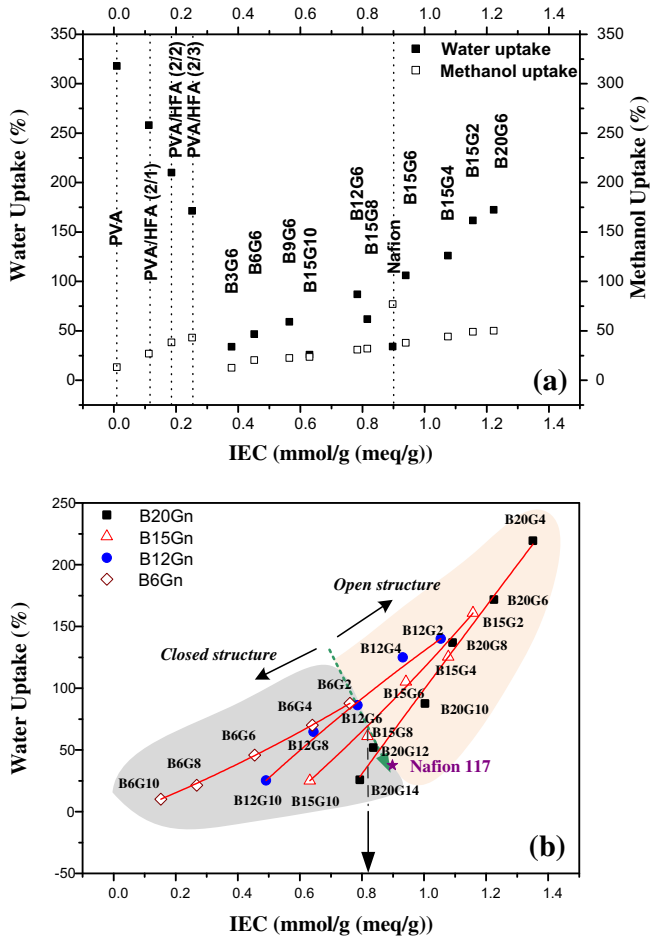

Fig. 6. (a) Water uptake and methanol uptake plotted as a function of IEC for polymer membranes. (b) Water uptake plotted as a function of IEC for the chemically cross-linked membranes in different binary reaction agents. Polymer composition of PVA/HFA = 2/2 (in mass).

cross-linking density is strongly increased when the bifunctional GA, ie., the aldehyde with alkyl chain as cross-linker.

It can summarize the above mention that the lowest water uptake is in the soaking medium of B15G10, but the IEC is less than Nafion®-117 (0.632 < 0.91). In addition, when the soaking medium of BASANa content adds to 15 wt.% or up to 20 wt.%, it can get a competitive extent of IEC. However, the water uptake also increases when the soaking medium of BASANa content adds to 15 wt.% or up to 20 wt.% because the mobility of ions in the water phase increase with increasing water content (volume) and build the high charge density in the membrane. As seen in Fig. 6a, the higher the mass ratio of BASANa content (=the higher IEC), together with other polar sites present in the membrane, the larger will be formation of ion clusters, which may allow greater sorption of water. The higher the mass ratio of GA content, the larger will be formation of cross-linking density, which may allow smaller sorption of water. We can also find that all the methanol uptake of the PVA/HFA (2/2) chemically cross-linked membranes in different binary reaction agents (MU = 12–49%) are much lower than Nafion®-117 (MU = 76.37%), even if embedded more sulfonic groups, this may be from the characteristic of PVA film. Moreover, we demonstrate additional binary reaction agents to achieve the sweet point where high IEC and low water uptake has at the same time. Fig. 6b shows the variation of water uptake plotted as a function of IEC for the chemically cross-linked membranes in different binary reaction agents. The membranes show a general trend that the water uptake increases with increasing IEC; it demonstrated that a distinct transition at which the way the membrane absorb water varied by the structure change upon changing the relative amount of sulfonic acid groups and crosslinking density. The slope of these four red lines of groups could indicate the practical number of water molecular per ionic site. The sweet point shown in graph is B20G14 as a binary cross-linking agent, where IEC = 0.79 meq g^{-1} is nudging value to Nafion®-117 and WU = 25 wt.% is lower than Nafion®-117 as well. In our previous study, we had showed experimentally that a similar transition of water uptake vs. IEC of our UV cured membrane [36]. It further showed this slope-changing transition was associated with a change in the network structure from close to open. The green dotted line indicated how to approach proper IEC value and preserve appropriate water uptake in the membrane through different chemical composition followed by the boundary structure of close and open. Generally, if the polymer membranes based on a series of higher hydrophilic groups—the slope will increase dramatically, causing the more aggregation of water with the strong interaction between them. Thus, if the more hydrophobic content in the network, it caused more reduction of water uptake drastically. This may be due to its sulfonic acid groups as "bound-water reservoirs" and reduce more free water in the membranes. In the following section, we will further discuss this phenomenon of the state of water in the membranes.

3.6. The state of water in the membranes

The state of water in particular has a strong influence on proton transport properties. Usually water in the membrane exists in two types: free water (FW) and bound water (BW) (non-freezing bound water + freezing bound water). When a small volume of water is absorbed into a polymer, the water molecules primarily associate with the polar and ionic groups present in the polymer chain. At a certain volume of absorbed water, the polar and ionic groups become saturated; the maximum volume of bound water is typically dependent on the polarity and the content of ionic groups in the polymer [44], thus this effect is known as electrostriction. Free water is not bound to the polymer and shows the same temperature and enthalpy of melting/crystallization as bulk water (i.e., 0 °C) [45]. Freezing bound water is defined as water that has a phase transition temperature less than 0 °C due to weak interaction such as hydrogen bonding with the hydrophilic groups in the polymer. Non-freezing bound water is defined as water that has no detectable phase transition from −73 °C to 0 °C because of strong interaction with the associate groups (i.e., sulfonic acid groups in the current case) of the polymer [46]. A series of water-swollen polymer membranes prepared in the present study containing a large amount of water in their networks. It demonstrated the water sorption characteristics and physicochemical properties depending not only on the water content but also on the state of water.

In this study, the DSC measurement was carried out to determine the amount of free water that is not bounded by hydrogen bonding. The fraction of free water in total water is approximately expressed as the ratio of the endothermic peak area at around 0 °C for the water-swollen membranes to the melting endothermic heat of fusion (334 Jg^{-1}) for pure water, using following equations:

$$m_{\text{free}} = \frac{\Delta H_{\text{free}}}{Q_{\text{melting}}} m_{\text{total}} \tag{12}$$

The heat of melting, ΔH_{free}, of the water was determined from the area below the DSC peak and from the weight of the water, and Q_{melting} was known to be $Q_{\text{melting}} = 334$ J g^{-1}. Bound water arising from hydrogen bonding with PVA chains and $-SO_3H$ and $-COOH$ groups is expressed as the difference between the total water and

the free water content. Table 3 shows the water content corresponding to the free and bound water in different polymer membranes. The water content of the PVA/HFA physically cross-linked membranes and chemically cross-linked PVA/HFA (2/2) membranes with BASANa/GA is found to be bound water more than free water, and this tendency is similar to Nafion®-117. However, the water content of the fresh PVA film is quite contrary. As shown in Table 3, the total water content decreases with increasing soaking medium of GA, due to the increased degree of cross-linking of the membranes. This makes the polymer structure more compact and rigid, and results in a decrease in the free volume capable of containing water molecules. While the bound water-to-total water ratio is nearly constant from membrane "PVA/HFA (2/2) in B15G2" to membrane "PVA/HFA (2/2) in B15G10". Besides, the total water content and bound water increase with increasing sodium medium of BASANa, indicative of an increase in the number of hydrophilic groups in the polymer by the cross-linking. This electrostriction phenomenon leads to a considerable reducing in entropy, since the bound water molecules have a restricted freedom of motion. Consequently, PVA blends with HFA and further produces thermal/chemical cross-linking networks which have good water management through its strongly or weakly bound to the polymer chain. In addition, BASANa cross-links to PVA network serving as "bound-water reservoirs" owing to its sulfonic acid groups. The free water and bound water contents are dependent on the total water content of the polymer membranes, indicating that the water states in the polymer are very different, depending on the polymer structure. It is reported that proton conductivity in membranes may be achieved via strongly bound water [47]. The ability of bound water to facilitate the transport of protons originates by generation of a continuous proton conductivity pathway.

3.7. Wide-angle X-ray diffraction (WAXD) measurement

Wide-angle X-ray is widely used a powerful tool to investigate the degree of crystallinity of polymer samples. In general, when a polymer contains a crystalline region, then the X-ray diffraction peaks are sharp, and their intensities are high, whereas for an amorphous polymer they are broad. Fig. 7 shows the wide-angle X-ray diffraction profiles for the pure PVA film, PVA/HFA (2/2) physically cross-linked polymer membrane and PVA/HFA (2/2) chemically cross-linked polymer membranes in different chemical cross-linking solution (B15G2 ~ B15G10). As can be seen, the pristine PVA film exhibits a semi-crystalline structure with a large peak at the scattering angle (2θ) around 20° corresponding to a mixture of (1 0 1) and (2 0 0) plane. Moreover, we can find that it associates with the convolution of an amorphous region and a crystalline region. It is well known that the crystallinity is high due to the hydroxyl groups in its side-chain. This is in agreement with the results reported elsewhere [44,48,49]. For the PVA/HFA (2/2) physically cross-linked polymer membrane, the peak position shifts to lower diffraction angles and the peak intensity greatly reduces, relating to small changes in intersegmented spacing. It was also clearly seen that the PVA/HFA (2/2) chemically cross-linked membranes in different binary agents greatly augmented the domain of amorphous region and decreased the degree of crystallinity. This demonstrates that the amorphous phase of the PVA/HFA (2/2) chemically cross-linked polymer membranes enhanced not only by introducing sulfonic acid groups to PVA chain but also by introducing GA quantity from 2 wt.% to 10 wt.%. It is well known that the hydroxyl groups of PVA physically crosslink with HFA to form ester bonds and chemically react with aldehydes to form acetal or semi-acetal linkages. Therefore, the number of hydroxyl groups from PVA molecules decreased, resulting in a decrease in crystallinity. Indeed, this physically and chemically crosslinking reaction on the PVA/HFA polymer membrane provides greater chemical, thermal and mechanical stabilities for DMFC applications.

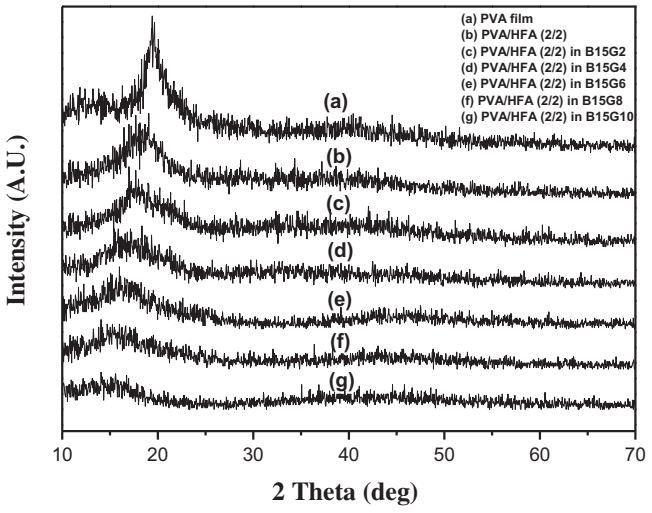

Fig. 7. WAXD spectra of the fresh PVA film, the PVA/HFA (2/2) physically cross-linked membrane and the PVA/HFA (2/2) chemically cross-linked membranes in different binary reaction agents for B15Gn (*n* from 2 wt.% to 10 wt.% of GA).

3.8. SAXS analysis and phase images

The tapping mode AFM phase images of the PVA/HFA (2/2) chemically cross-linked polymer membranes in different binary reaction agents from B15G2 to B15G10 under ambient conditions were recorded on a 500 nm × 500 nm size scale to investigate the polymer nanodomains as well as the ionic nanochannels (Fig. 8b). All samples show nanophase separated morphology as indicated by the dark and bright regions; this phase lag of changing phenomenon reflect changes of some physical characteristics, including of hardness, friction, composition, viscoelasticity and etc. The dark regions in the images are attributed to the hydrophilic sulfonate acid groups containing water, i.e., standing for its soft structure of proton conductive pathway; however, the bright regions in the images are attributed to the hydrophobic polymer matrix, corresponding to a hard structure endowing the membrane with mechanical strength [50,51]. The cross-linked membrane in binary reaction agents for B15G10 exhibits many segregated ionic domains in the continuous hydrophobic polymer matrix, thus, the proton conducts difficultly through the hydrated ionic domains. On the contrary, with lower degree of chemical cross-linking having more connective ionic domains and the nanophase separation becomes more palpable.

Fig. 8a shows the SAXS spectra of the PVA/HFA (2/2) chemically cross-linked membranes in binary reaction agent for B12G6 and B15G8 in comparison with Nafion®-117, and all are corresponding to its AFM phase image, this tendency is chosen from the green dotted line of Fig 6b. We could determine the vector q ($=2\pi/d$) denoting the inverse distance between the microdomains from the SAXS profiles [52]. As mentioned previously, the formation of hydrophilic ionic channels is achieved mainly by the arrangement of hydrophilic polymeric groups due to the hydrogen bonding formation during the thermal treatment. Typical hydrophobic/hydrophilic separation lengths were calculated from the broad peak maximum (ionomer peak) using the Bragg relation and summarized in Table 4. The size (d) of the separation of channels (center-to-center) in Nafion®-117 (i.e. 3.6 nm) is relatively smaller than that in the PVA/HFA (2/2) chemically cross-linked membrane in binary reaction agent for B12G6 (i.e. 10.13 nm) and B15G8 (i.e. 7.31 nm),

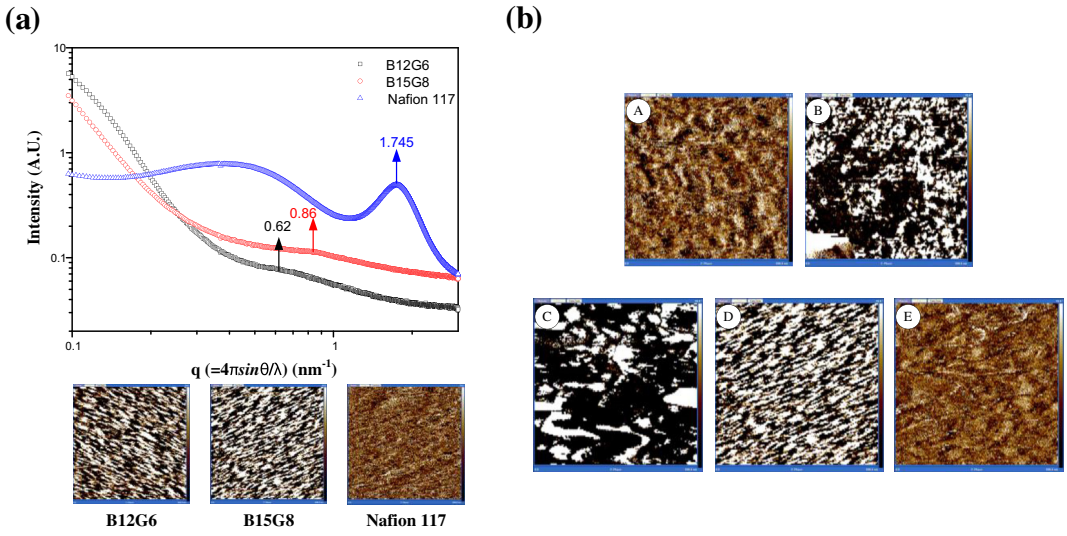

Fig. 8. (a). SAXS spectra of the PVA/HFA (2/2) chemically cross-linked membranes in binary reaction agent for B12G6 and B15G8 compared with Nafion®-117, all corresponding to its AFM phase image. (b). The AFM phase image of the PVA/HFA (2/2) chemically cross-linked membranes in different binary reaction agents for A (B15G2), B (B15G4), C(B15G6), D (B15G8) and E (B15G10), respectively. Each image frame is 500 nm × 500 nm, and phase scales are 0–10°.

when the membranes are wetted with deionized water. These correlation peaks systematically shifts to much higher q values indicated with increasing sulfonic acid groups in order to close IEC of Nafion®-117 as well as maintain its water content. In other words, highly sulfonated polymers and moderate cross-linking could control water content with highly dispersion which corresponds to more narrow water structures. This implication in here is that being more IEC values without causing the ramification of spoiling the separation of hydrophobic/hydrophilic, hence the proper cross-linking support its pore size's structure and get more narrow ion clusters without sacrificing the proton conductivity.

3.9. Proton conductivity and methanol permeability

Fig. 9 shows proton conductivity (σ) and methanol permeability through the cross-linked membranes as a function of the IEC, which have the exponent relationship. The more cross-linkable moiety is introduced, the lower are the proton conductivity and methanol permeability in the cross-linked membranes with the same degree of sulfonation (DS). It is more significant to have a transition change in slope of permeability vs. IEC. A distinct in decreasing crosslinking density would cause to exhibit an open structure of network while IEC > 0.82 meq g^{-1} exhibits a close structure of highly crosslinked network while IEC < 0.82 meq g^{-1}. The results also correspond with the previous phase image results and are similar to the water uptake property that increasing cross-linker density would reduce the size of the ionic channels, resulting in the restrained and bridled conveyance of protons and methanol. However, the methanol permeability is not only substantially lower than that of a commercial Nafion®-117 membranes (the range between 6×10^{-6} cm^2 s^{-1} to 4×10^{-8} cm^2 s^{-1}) but the proton conductivity is also within reasonable values compared with Nafion®-117

Table 4
The characteristic hydrophobic/hydrophilic separation lengths.

Membranes		q (nm^{-1})	d (nm)
PVA/HFA (2/2) in B12G6	Wetted (in H_2O)	0.62	10.13
PVA/HFA (2/2) in B15G8	Wetted (in H_2O)	0.86	7.31
Nafion®-117	Wetted (in H_2O)	1.745	3.6

$d = 2\pi/q$ (q: scattering vector (nm^{-1}); d: interplanar distance (nm)).

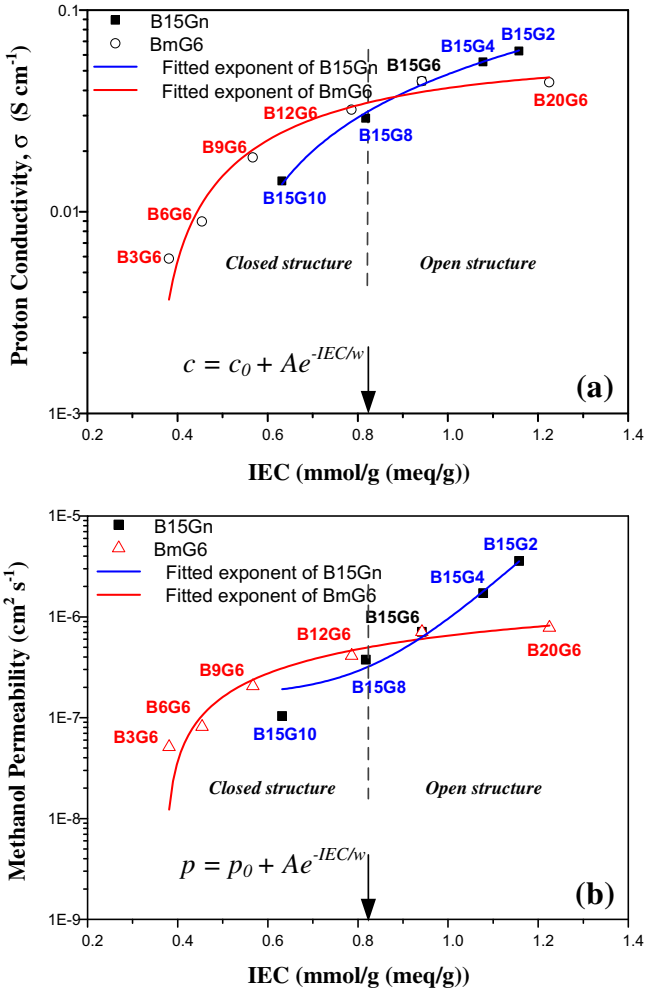

Fig. 9. Proton conductivity and methanol permeability of the chemically cross-linked membranes in different binary reaction agents for B15Gn (n from 2 wt.% to 10 wt.% of GA) and BmG6 (m from 3 wt.% to 20 wt.% of BASANa) as a function of IEC. Polymer composition of PVA/HFA = 2/2 (in mass).

Table 5
Mechanical properties of the PVA/HFA (2/2) chemically cross-linked membranes in different binary reaction agents for B15Gn (*n* from 2 wt.% to 10 wt.%) compared with that of Nafion®-117.

Membranes	Young's modulus (MPa%$^{-1}$)	Tensile strength (kg mm^{-2})	Elongation (%)	Bending test
PVA/HFA (2/2) in B15G2	21.5	1.8	23.6	Level V
PVA/HFA (2/2) in B15G4	26.7	2.1	19.5	Level V
PVA/HFA (2/2) in B15G6	28.5	2.4	16.3	Level V
PVA/HFA (2/2) in B15G8	30.6	2.8	13.7	Level V
PVA/HFA (2/2) in B15G10	33.8	3.2	12.4	Level IV
Nafion®-117	23.4	2.3	12.2	Level V

(5.14×10^{-2} S cm^{-1}) [36,43]. From the plot we could find the B15Gn membrane's methanol permeability is more sensitive than its proton conductivity when reducing cross-linker density from close structure to open structure. This means cross-linker is the crux for controlling and governing methanol crossover. However, this would not affect the proton exchange distinctly if the degree of sulfonation (DS) is proper and the "bound-water reservoirs" are sufficient for facilitating the transport of protons that originates from the generation of a continuous proton conductivity pathway. Theoretically, when more degree of sulfonation is induced, the higher are proton conductivity and methanol permeability in the cross-linked membranes with the same degree of cross-linking. Nevertheless, these two properties seen from the graph demonstrated that the increase becomes slow in the higher DS because of their strong affinity toward water contributing to the high mobility of free ions. Thus, diluting and dispersing the proton diffusivity and indirectly influence its methanol diffusivity. Accordingly, these hydrophilic areas formed around the cluster of side chains lead to absorption of water, enabling easy proton transfer [53]. We can expect a series reduction of extra free water in the PVA polymer membranes, resulting in extremely low methanol crossover. Nafion, despite forming highly packed nanostructured hydrophilic channels, actually consists of low-molecular-weight sulfonated perfluoro-polymer molecules which can be easily solvated by methanol solution because of their relatively short and low density of hydrophobic groups. Consequently, methanol crossover is high in Nafion. It is also believed from graph that a better methanol rejecter where the presence of more HFA as cross-linker could also lead to improvement in membrane chemical stability.

3.10. Mechanical property

Besides its high proton conductivity, a proton exchange membrane (PEM) should serve several functions such as good hydrolytic stability, good oxidative stability, reasonable thermal stability and appropriate mechanical property. It should have even lower methanol permeability if methanol is used as fuels of PEM fuel cells. The mechanical properties of chemically cross-linked PVA/HFA blend membranes were tested for the tensile strength and tensile elongation and, the results are listed in Table 5. All tested samples are ductile. We noted that the tensile strength increased when increasing the mass ratio of the hydrophobicizer (i.e., GA). However, the elongation increased not only by reducing the mass ratio of the hydrophobicizer but also by increasing the mass ratio of HFA blended in the polymer PVA. This strength may be accounted for, in large part, by constraints posed by entanglements formed between the bifunctional GA during chemically cross-linked reaction and the fluoric-type of HFA blends inside the PVA during the physically cross-linked reaction. In brief, the PVA/HFA possess physically and chemically cross-linked membranes show good mechanical properties compared to Nafion®-117 owing to high flexibility of the HFA, which allows easy relaxation of the polymer chains. Besides, we also test the bending properties of polymer membranes as is shown in Table 5.

3.11. Selectivity (Φ)

High methanol crossover is an enormous obstacle for membranes in fuel cell applications such as DMFC. So a good performance needs high proton conductivity and low methanol permeability. Therefore, the ratio of proton conductivity to methanol permeability or selectivity (Φ) is, to some extent, more important than the pure methanol permeability. The higher the Φ value is, and then one can expect better performance. It can be noticed from Fig. 10, selectivity (Φ) values of the PVA/HFA (2/2) chemically cross-linked membranes were all higher than that of Nafion®-117. In addition, different binary reaction agents cased a variety of IEC, WU, σ, and methanol permeability which contributed to different selectivity (Φ) values.

3.12. Hydrolytic stability and oxidative stability

To evaluate the cross-linked membranes, time dependent measurements of the proton conductivity and the IEC at an elevated temperature of 60 °C for a week were carried out. The hydrolytic water test is a simple initial accelerated test to evaluate the possibility as membrane materials for fuel cell. Choosing 60 °C water test is in order to prove the stability for low temperature DMFC in general surroundings. Before and after 60 °C water test, the proton conductivity and the IEC values are listed in Table 6. Although the proton conductivity and IEC values only decrease slightly (change less than 11%) in low degree of cross-linking, perhaps due to partial decomposition during the 60 °C water test, the membranes maintain adequate proton conductivity and IEC values after the 60 °C water test. In addition, the membranes in high degree of cross-linking show an excellent hydrolytic stability for a long time without any decrease in the proton conductivity and the IEC (change less than 4%). The changing proton conductivity with time

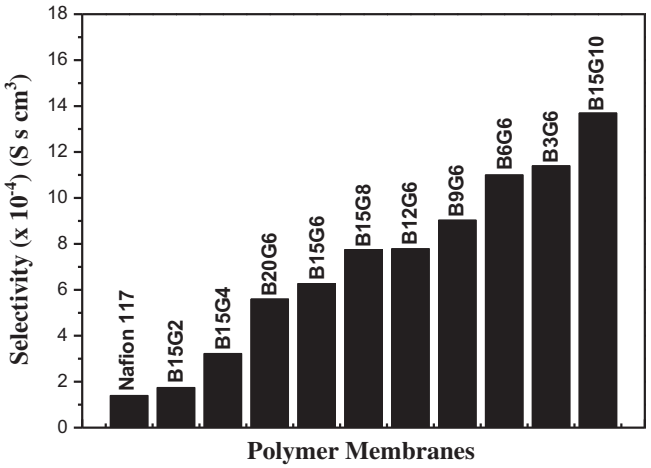

Fig. 10. The selectivity of the PVA/HFA (2/2) chemically cross-linked membranes in different binary reaction agents for BmGn compared with those of Nafion®-117.

Table 6
The hydrolytic stability of the PVA/HFA (2/2) chemically cross-linked membranes in different binary reaction agents for B15Gn (*n* from 2 wt.% to 10 wt.%).

Membranes	IEC (mmol g^{-1} (meq g^{-1}))			Proton conductivity (S cm^{-1})		
	Before 60 °C water test	After 60 °C water test	Change (%)	Before 60 °C water test	After 60 °C water test	Change (%)
PVA/HFA (2/2) in B15G2	1.158	1.043	9.931	0.0627	0.0563	10.236
PVA/HFA (2/2) in B15G4	1.078	0.991	8.071	0.0554	0.0508	8.224
PVA/HFA (2/2) in B15G6	0.942	0.879	6.688	0.0444	0.0419	5.647
PVA/HFA (2/2) in B15G8	0.818	0.787	3.790	0.0291	0.0281	3.431
PVA/HFA (2/2) in B15G10	0.632	0.621	1.788	0.0142	0.0139	2.043

Table 7
The oxidative stability of the PVA/HFA (2/2) chemically cross-linked membranes in different binary reaction agents for B15Gn (*n* from 2 wt.% to 10 wt.%). Times were recorded from commencement to break of samples in Fenton's reagent.

Membranes	Oxidative time (min)
PVA/HFA (2/2) in B15G2	47
PVA/HFA (2/2) in B15G4	56
PVA/HFA (2/2) in B15G6	66
PVA/HFA (2/2) in B15G8	74
PVA/HFA (2/2) in B15G10	82

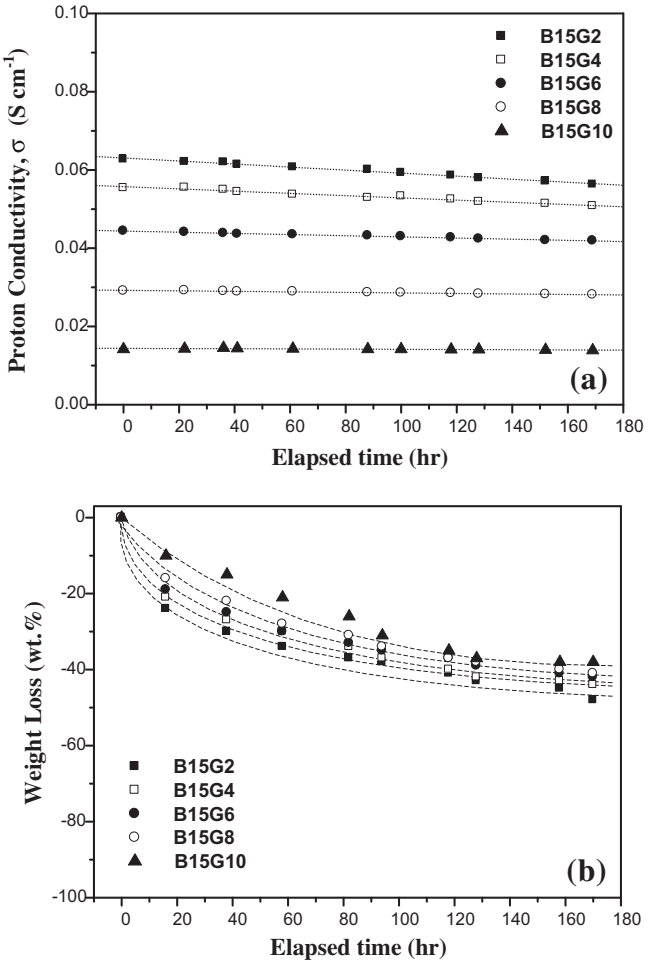

Fig. 11. (a). Time course of the proton conductivity for the PVA/HFA (2/2) chemically cross-linked membranes in different binary reaction agents for B15Gn (n from 2 wt.% to 10 wt.% of GA). (b). Oxidative stability of the PVA/HFA (2/2) chemically cross-linked membranes in different binary reaction agents for B15Gn (n from 2 wt.% to 10 wt.% of GA). Fenton's durability experiment of those membranes in Fenton's reagent (i.e., 10 wt.% H_2O_2 solution containing 5 ppm $FeSO_4$) at room temperature.

course can be observed clearly from Fig. 11a. Generally, membranes with high IEC values tend to yield large WU and thus have a poor water stability [33]. In fact, all the membrane samples exhibited a good hydrolytic stability without any changes in original appearance, flexibility, and tenacity even after they had been immersed in 60 °C water more than a week, although most of their WU and IEC are higher than that of Nafion®-117.

We have also performed an oxidative stability test in Fenton's reagent (i.e., 10 wt.% H_2O_2 solution containing 5 ppm $FeSO_4$) for the cross-linked membranes. Fenton's reagent was widely used for the stability evaluation of perfluorosulfonic acid (PFSA) PEMs and other polymer membranes. The principal degradation mechanism of the polymer membranes in Fenton's reagent has been fully investigated and discussed in the literature [54]. The aqueous solution containing H_2O_2 and $FeSO_4$ forms OH radicals inside the solution, and the OH• radical may attack the polymer and decompose it [55]. However, OH radical lifetimes are short and the OH• radical cannot penetrate or diffuse into the chemically cross-linked PVA/HFA membranes. This may be the reason for the much improved oxidative stability of the PVA/HFA chemically cross-linked membranes. The cross-linking structure may also contribute to the stability. The calculated results with the chemically cross-linked PVA/HFA membranes of oxidative time and weight loss with elapsed time are shown in Table 7 and Fig. 11b, respectively. Therefore, it is believed that the PVA/HFA chemically cross-linked membranes have moderate hydrolytic stability and oxidative stability, which could be successfully utilized in real fuel cell applications operated under relatively mild conditions.

4. Conclusions

This work focused on the development of low cost methanol resistant proton exchange membranes (PEMs) for direct methanol fuel cell applications. The PEMs were formulated as a physically and chemically PVA/HFA (PVA/hexafluoroglutaric acid) blending membranes with BASANa (Benzenesulfonic acid sodium salt) and GA (Glutaraldehyde) as binary reaction agents. This cross-linked membranes acquired dual functionalities, i.e., effective proton transport between hydrophilic groups (−SO_3H) interconnecting with PVA chains, resulting in proton conductivity of the order of 10^{-3}–10^{-2} S cm^{-1}, high IEC, and good water management. Moreover, the inhibited methanol passage in the continuous amphiphilic matrix results, in methanol permeability of the order 10^{-7}–10^{-8} cm^2 s^{-1}, which is average about 10 times smaller than that of Nafion®-117. This may be because of the water structure inside the polymer membranes as a result of suppression of swelling and may control the free water content in the membranes. It also concluded that the IEC value was an important parameter affecting the performance of resulting membrane (WU, conductivity and methanol permeability). Based on the above analysis, a transition from a closed network structure to an open one was observed. A thorough examination of membrane stability is also warranted to test the general applicability of these materials in DMFCs. Therefore, these

kinds of membranes have the potential for practical use not only in high-energy-density devices but also in automobile applications.

Acknowledgments

The financial support from the National Science Council of Taiwan under contract no. NSC95-2218-E-002-040, NSC96-2221-E-002-145, and from the Industrial Technology Research Institute of Taiwan is greatly appreciated.

References

[1] A. Aramata, I. Toyoshima, M. Enyo, Electrochim. Acta 37 (1992) 1317.
[2] D. Sangeetha, Eur. Polym. J. 41 (2005) 2644.
[3] Y.A. Elabd, E. Napadensky, J.M. Sloan, D.M. Crawford, C.W. Walker, J. Memb. Sci. 217 (2003) 227.
[4] Y. Yang, F. Mikes, Y. Koike, Y. Okamoto, Macromolecules 37 (2004) 7918.
[5] R.W. Kopitzke, C.A. Linkous, H.R. Anderson, G.L. Nelson, J. Electrochem. Soc. 147 (2000) 1677.
[6] C.J. Zhao, X.F. Li, Z. Wang, Z.Y. Dou, S.L. Zhong, H. Na, J. Memb. Sci. 280 (2006) 643.
[7] G.P. Robertson, S.D. Mikhailenko, K.P. Wang, P.X. Xing, M.D. Guiver, S. Kaliaguine, J. Memb. Sci. 219 (2003) 113.
[8] Y. Gao, G.P. Robertson, M.D. Guiver, S.D. Mikhailenko, X. Li, S. Kaliaguine, Macromolecules 37 (2004) 6748.
[9] K. Miyatake, H. Zhou, T. Matsuo, H. Uchida, M. Watanabe, Macromolecules 37 (2004) 4961.
[10] Y. Yin, J.H. Fang, Y.F. Cui, K. Tanaka, H. Kita, K. Okamoto, Polymer 44 (2003) 4509.
[11] P. Staiti, F. Lufrano, A.S. Arico, E. Passalacqua, V. Antonucci, J. Memb. Sci. 188 (2001) 71.
[12] V. Deimede, G.A. Voyiatzis, J.K. Kallitsis, L. Qingfeng, N.J. Bjerrum, Macromolecules 33 (2000) 7609.
[13] J.W. Rhim, C.K. Yeom, S.W. Kim, J. Appl. Polym. Sci. 68 (1998) 1717.
[14] J.M. Gohil, A. Bhattacharya, P. Ray, J. Polym. Res. 13 (2006) 161.
[15] M.L. Zhai, F. Yoshii, T. Kume, K. Hashim, Carbohyd Polym. 50 (2002) 295.
[16] T.M.R. Miranda, A.R. Goncalves, M.T.P. Amorim, Polym. Int. 50 (2001) 1068.
[17] S.G. Kumbar, T.M. Aminabhavi, J. Appl. Polym. Sci. 84 (2002) 552.
[18] W.Y. Chiang, Y.H. Lin, J. Appl. Polym. Sci. 86 (2002) 2854.
[19] J. Ruiz, A. Mantecon, V. Cadiz, J. Appl. Polym. Sci. 81 (2001) 1444.
[20] K. Kumeta, I. Nagashima, S. Matsui, K. Mizoguchi, J. Appl. Polym. Sci. 90 (2003) 2420.
[21] R.Y.M. Huang, J.J. Shieh, J. Appl. Polym. Sci. 70 (1998) 317.
[22] V. Gimenez, A. Mantecon, J.C. Ronda, V. Cadiz, J. Appl. Polym. Sci. 65 (1997) 1643.
[23] M. Krumova, D. Lopez, R. Benavente, C. Mijangos, J.M. Perena, Polymer 41 (2000) 9265.
[24] E. Da Silva, L. Lebrun, M. Metayer, Polymer 43 (2002) 5311.
[25] J. Yu, C.H. Lee, W.H. Hong, Chem. Eng. Process. 41 (2002) 693.
[26] N.A. Peppas, P.J. Hansen, J. Appl. Polym. Sci. 27 (1982) 4787.
[27] S.D. Xiao, R.Y.M. Huang, X.S. Feng, J. Memb. Sci. 286 (2006) 245.
[28] B.S. Pivovar, Y.X. Wang, E.L. Cussler, J. Memb. Sci. 154 (1999) 155.
[29] J.W. Rhim, H.B. Park, C.S. Lee, J.H. Jun, D.S. Kim, Y.M. Lee, J. Memb. Sci. 238 (2004) 143.
[30] D.S. Kim, M.D. Guiver, S.Y. Nam, T. Il Yun, M.Y. Seo, S.J. Kim, H.S. Hwang, J.W. Rhim, J. Memb. Sci. 281 (2006) 156.
[31] M.S. Kang, J.H. Kim, J. Won, S.H. Moon, Y.S. Kang, J. Memb. Sci. 247 (2005) 127.
[32] J.L. Qiao, T. Hamaya, T. Okada, Chem. Mater. 17 (2005) 2413.
[33] J.L. Qiao, T. Hamaya, T. Okada, J. Mater. Chem. 15 (2005) 4414.
[34] J.L. Qiao, T. Hamaya, T. Okada, Polymer 46 (2005) 10809.
[35] M.M. Nasef, N.A. Zubir, A.F. Ismail, M. Khayet, K.Z.M. Dahlan, H. Saidi, R. Rohani, T.I.S. Ngah, N.A. Sulaiman, J. Memb. Sci. 268 (2006) 96.
[36] C.A. Dai, C.P. Liu, Y.H. Lee, C.J. Chang, C.Y. Chao, Y.Y. Cheng, J. Power Source 177 (2008) 262.
[37] Y. Yin, Y. Suto, T. Sakabe, S.W. Chen, S. Hayashi, T. Mishima, O. Yamada, K. Tanaka, H. Kita, K. Okamoto, Macromolecules 39 (2006) 1189.
[38] S. Panero, P. Fiorenza, M.A. Navarra, J. Romanowska, B. Scrosati, J. Electrochem. Soc. 152 (2005) A2400.
[39] R.L. Guo, C.L. Hu, B. Li, Z.Y. Jiang, J. Memb. Sci. 289 (2007) 191.
[40] R.Y.M. Huang, C.K. Yeom, J. Memb. Sci. 58 (1991) 33.
[41] J.H. Kim, B.R. Min, K.B. Lee, J.G. Won, Y.S. Kang, Chem. Commun. (2002) 2732.
[42] M.A. Vargas, R.A. Vargas, B.E. Mellander, Electrochim. Acta 45 (2000) 1399.
[43] M.H. Jeong, K.S. Lee, J.S. Lee, Macromolecules 42 (2009) 1652.
[44] D.S. Kim, H.B. Park, J.W. Rhim, Y.M. Lee, J. Memb. Sci. 240 (2004) 37.
[45] A. Higuchi, T. Iijima, Polymer 26 (1985) 1833.
[46] H.Q. Pei, L. Hong, J.Y. Lee, Langmuir 23 (2007) 5077.
[47] A. Siu, J. Schmeisser, S. Holdcroft, J. Phys. Chem. B 110 (2006) 6072.
[48] C.C. Yang, S.J. Lin, J. Appl. Electrochem. 33 (2003) 777.
[49] S.Y. Nam, H.J. Chun, Y.M. Lee, J. Appl. Polym. Sci. 72 (1999) 241.
[50] F. Yan, S.M. Yu, X.W. Zhang, L.H. Qiu, F.Q. Chu, J.B. You, J.M. Lu, Chem. Mater. 21 (2009) 1480.
[51] J.H. Pang, H.B. Zhang, X.F. Li, Z.H. Jiang, Macromolecules 40 (2007) 9435.
[52] J. Won, H.H. Park, Y.J. Kim, S.W. Choi, H.Y. Ha, I.H. Oh, H.S. Kim, Y.S. Kang, K.J. Ihn, Macromolecules 36 (2003) 3228.
[53] B. Smitha, S. Sridhar, A.A. Khan, Macromolecules 37 (2004) 2233.
[54] A. Bosnjakovic, S. Schlick, J. Phys. Chem. B 108 (2004) 4332.
[55] T. Yamaguchi, H. Zhou, S. Nakazawa, N. Hara, Adv. Mater. 19 (2007) 592.